Journal of Quantitative Spectroscopy & Radiative Transfer 109 (2008) 1219–1233

Journal of Quantitative Spectroscopy & Radiative Transfer

www.elsevier.com/locate/jqsrt

A line list of allowed and forbidden rotational transition intensities for water

Lorenzo Lodi[a], Jonathan Tennyson[a,*]

[a]*Department of Physics and Astronomy, University College London, London WC1E 6BT, UK*

Received 21 July 2007; received in revised form 24 September 2007; accepted 25 September 2007

Abstract

Pure rotational lines are important for monitoring water concentrations in many environments both in space and on earth. A list of line intensities of rotational transitions for $H_2{}^{16}O$ is calculated using variational nuclear-motion wave functions and an *ab initio* dipole moment surface. This methodology should be equally reliable for both allowed and forbidden rotational transitions. Extensive comparisons are made with available intensity data for these transitions including the HITRAN and JPL databases. Problems are identified with some of these data. A list of 555 allowed and 846 forbidden rotational transition lines within the ground vibrational state is made available.

Keywords: Water vapour; Line intensities; Atmospheric physics

1. Introduction

Monitoring water vapour columns is a major activity in atmospheric physics, astrophysics and many other areas [1]. Indeed, entire atmospheric and space satellite missions have been launched with this as their major goal [2–4]. The reliability of the underling spectroscopic data upon which this activity is based is therefore crucial to the success of these missions.

The rotational spectrum of $H_2{}^{16}O$ is experimentally well studied for transition energies but much less so for absolute intensities (e.g. [5–10]). It is possible to classify lines of the water rotational spectrum into allowed and forbidden lines (see below for a precise definition of these terms); in atmospheric, and other, applications the allowed lines are generally saturated and are therefore not useful for monitoring purposes. The weaker forbidden lines, which generally lie at shorter wavelengths than the allowed ones, can therefore provide a useful tool with which to study water vapour.

Rotational spectra can be modelled usually very accurately using effective Hamiltonians based on perturbation theory [11–13]. In this work we use instead rotation–vibration wave functions defined from the variational principle rather than perturbation theory [14]. These wave functions are calculated with the minimum number of approximations [15] and therefore should not bias one set of transitions over another.

*Corresponding author.
E-mail address: j.tennyson@ucl.ac.uk (J. Tennyson).

0022-4073/$ - see front matter
doi:10.1016/j.jqsrt.2007.09.015

The original aim in undertaking this study was to check that the available perturbation theory based calculations, and indeed laboratory measurements, were of equal validity for the forbidden lines. In practise we found that data on pure rotational lines of water was in a less satisfactory state than we had anticipated. For this reason we decided to provide a complete listing of the pure rotational lines of water with intensities greater than 10^{-28} cm/molecule at 296 K.

Neglecting weak nuclear-spin coupling effects [16], the rotation–vibration energy levels of water have the following rigorous quantum numbers: rotational angular momentum, J, parity, p, and a further quantum number specifying whether the nuclear-spin state of the hydrogen nuclei is ortho or para. Electric–dipole transitions can in principle occur between any states within either the ortho or para networks for which $\Delta J = \pm 1$ and $\Delta p = 0$ or $\Delta J = 0$ and $\Delta p = 1$. Naturally not all these transitions are equally strong and it is usual to label the states in terms of approximate quantum numbers, from which it is easy to infer an approximate notion of the transition strength. For purely rotational states the approximate quantum numbers are the projection of the angular momentum on the A-axis, K_a, and on the C-axis, K_c. In terms of these the rigorous selection rules for pure rotational transitions correspond to transitions for which ΔK_a and ΔK_c are both odd. Analysis based on perturbation theory suggests that the strongest rotational transitions are those for which $\Delta K_a = \pm 1$ and $\Delta K_c = \pm 1$. Following the usual practise in atomic physics [17], we describe these transitions as allowed and the generally weaker transitions, for which ΔK_a and/or ΔK_c change by more than 1, as forbidden.

2. Calculation details

Nuclear-motion wave functions and transition intensities for J up to 15 were computed with the software suite DVR3D [18] using the FIS3 semi-empirical potential energy surface (PES) of Shirin et al. [19] and the recent *ab initio* CVR dipole moment surface (DMS) [20]. Basis sets developed by Barber et al. [21] in the course of their calculation of the comprehensive BT2 line list were used for all calculations. These are large enough to remove all issues to do with convergence for the low-lying states considered here. Intensities were generated at the HITRAN [22] reference temperature of 296 K. All computations were performed using a Pentium IV 3 GHz PC with 3 GB of RAM running 32-bit Linux and took altogether about two weeks.

Given that the nuclear motion calculations are highly converged, the accuracy of our approach depends only on the accuracy of the underlying PES used (and the associated corrections to the Born-Oppenheimer approximation [23] used) and the accuracy of the DMS. Although some transition intensities do show strong sensitivity to the underlying PES [20,24], room temperature transitions within the (0 0 0) band only involve rotational levels with low energies (up to about 5600 cm^{-1}) which, in turn, are essentially determined by the corresponding low-energy portion of the PES used. All modern energy surfaces describe accurately the low-energy region, so a strong sensitivity of transition intensities to the PES used is not expected. As a check we calculated a second set of nuclear-motion wavefunctions using a different PES, the recent CVRQD fully *ab initio* PES of Barletta et al. [15,25]. The result of the analysis is that, in consequence of the change of the nuclear-motion wavefunctions, line intensities generally change by less than 0.5%.

The quality of the energy surface can be partially evaluated by comparing computed transition wavenumbers with experimental ones. In most situations the measured wavenumbers are orders of magnitude more accurate than our computed ones. The reported wavenumbers from JPL and HITRAN always agree to better than 0.01 cm^{-1} and typically to about 0.0002 cm^{-1}. Our computed wavenumbers differ from experiment at worst by 0.10 cm^{-1} and typically by about 0.05 cm^{-1}. Such errors are 1 part in several thousand which is much higher accuracy than is aspired to for the line intensities. This analysis suggests that the major source of error in our calculations will be the DMS. The dependence of our results on the DMS will be discussed further below.

At 296 K we find 555 allowed and 846 forbidden rotational transitions within the ground, (0 0 0), vibrational band state that are stronger than 10^{-28} cm/molecule. Our calculated data for these transitions have been placed in the electronic archive. There are then many other weaker forbidden lines. Fig. 1 gives a graphical representation of the distribution of the transitions by intensity and transition wavenumber. At 296 K the most intense lines lie around 250 cm^{-1} with intensities then falling exponentially with the transition wavenumber (this is due to a Boltzmann factor $\mathrm{e}^{-E_{\mathrm{lower}}/k_{\mathrm{B}}T}$ in the intensity formula, reported as Eq. (4)). At

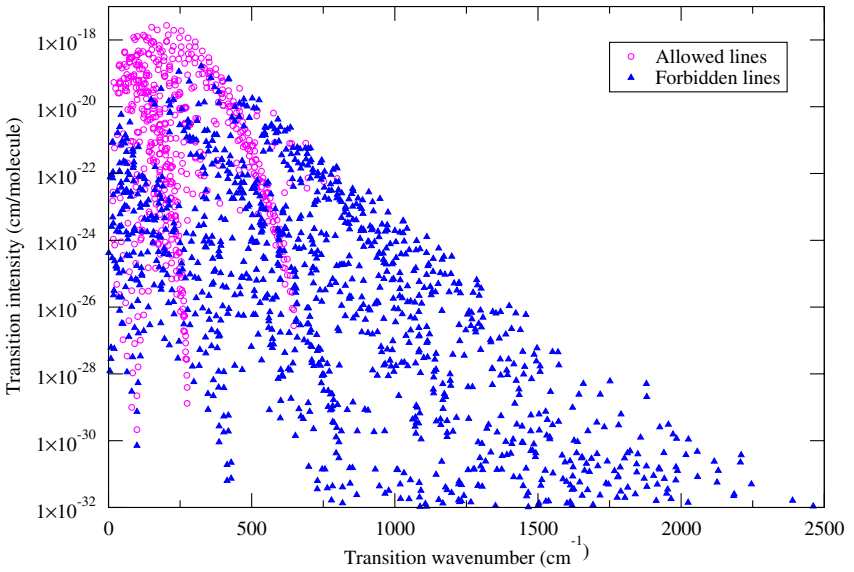

Fig. 1. Plot of calculated transition intensity at 296 K against transition wavenumber for transitions within the (0 0 0) vibrational band.

higher temperatures there is significantly increased absorption due to rotational transitions at higher wavenumbers [26].

Fig. 1 distinguishes between allowed and forbidden transitions. In general the allowed lines are the strongest. However, below intensities of about 10^{-20} cm/molecule there are many important forbidden lines.

3. Analysis

In order to understand our results and, in particular, to assess their reliability we made comprehensive comparisons with the available data on the intensities of pure rotational lines. We identified six key data sources which we compared against:

(1) lines from the HITRAN 2004 database [22,27],
(2) lines from the JPL catalogue [28–33],
(3) experimental lines from Rinsland et al. [6],
(4) experimental lines from Brown and Plymate [7],
(5) experimental lines from Toth [9,34],
(6) theoretical lines calculated from the BT2 [21] line list.

We also compare our results with effective Hamiltonian calculations due to Coudert [12].

Excluding the comprehensive BT2, there are for $J \leqslant 15$ a total of 1919 lines present in at least one of the data compilations above (555 allowed and 1364 forbidden), all of which could be matched with calculated lines. Table 1 presents a comparison of the published data with our calculations. For this purpose we have arbitrarily divided the transitions according to intensity (I in cm/molecule) into strong ($I > 10^{-20}$), medium ($10^{-24} < I \leqslant 10^{-20}$), weak ($10^{-28} < I \leqslant 10^{-24}$) and very weak ($I < 10^{-28}$). The very weak transitions are largely outside the scope of this study.

Our calculations give precisely 50 lines with intensity greater than 10^{-28} cm/molecule which do not appear in either the HITRAN or JPL databases. These lines are all forbidden and lie in the 996–1507 cm^{-1} region, usually not associated with pure rotational transitions of water. At 296 K the strongest omitted transition is $14_{8,7}-13_{1,12}$ calculated to lie at 1422.61 cm^{-1} with an intensity of 6.6×10^{-28} cm/molecule.

Table 1
Comparison of line intensities, I in cm/molecule, within the (0 0 0) vibrational band by intensity window

Source	$I > 10^{-20}$						$10^{-24} < I \leqslant 10^{-20}$						$10^{-28} < I \leqslant 10^{-24}$						$I < 10^{-28}$					
	Allowed			Forbidden			Allowed			Forbidden			Allowed			Forbidden			Allowed			Forbidden		
	n_p	$\langle\varrho\rangle_g$	σ	n_p	$\langle\varrho\rangle_g$	σ	n_p	$\langle\varrho\rangle_g$	σ	n_p	$\langle\varrho\rangle_g$	σ	n_p	$\langle\varrho\rangle_g$	σ	n_p	$\langle\varrho\rangle_g$	σ	n_p	$\langle\varrho\rangle_g$	σ	n_p	$\langle\varrho\rangle_g$	σ
BT2 [21]	187	1.003	0.000	24	1.003	0.000	234	1.003	0.000	370	1.004	0.001	128	1.003	0.000	452	1.007	0.003	2	1.004	0.000	517	1.007	0.293
HITRAN [22]	187	1.021	0.010	24	1.016	0.007	234	1.037	0.017	370	1.007	0.019	123	1.035	0.017	347	0.990	0.313	0		–	4	0.004	0.840
JPL [33]	187	1.007	0.009	24	0.999	0.010	234	0.997	0.021	363	0.999	0.035	128	0.974	0.038	318	1.008	0.102	6	0.939	0.011	102	0.975	0.798
Brown and Plymate [7]	62	0.978	0.023	2	0.954	0.031	0		–	0		–	0		–	0		–	0		–	0		–
Toth [9,34]	0		–	0		–	9	1.034	0.021	138	1.021	0.036	6	1.012	0.075	98	0.932	0.328	0		–	0		–
Rinsland et al. [6]	0		–	0		–	0		–	32	1.027	0.020	0		–	3	1.007	0.034	0		–	0		–

$\langle\varrho\rangle_g$ is the geometric mean of the ratios, σ the standard deviation of the natural logarithm of the ratios and n_p the number of lines falling in a specific intensity window. See text for precise definitions.

Some care should be used when comparing line intensities I between two data sets A and B. This is because absolute values considered may cover more than ten orders of magnitude and because for both calculations and experiments systematic errors may be present, leading to a few cases where I_A and I_B differ greatly (so-called outliers). The presence of a few outliers can potentially render devoid of meaning quantities such as averages or standard deviations if they are taken in a naive way.

We found the most useful quantities to be the geometric mean of the ratios of the intensities:

$$\langle \varrho \rangle_{\mathrm{g}} = \left(\prod_i \varrho_i \right)^{1/N} = \exp\left(\frac{1}{N} \sum_i \ln(\varrho_i) \right) \tag{1}$$

and the associated standard deviation of natural logarithm of the ratios

$$\sigma = \sqrt{\frac{1}{N} \sum_i [\ln(\varrho_i) - \ln(\langle \varrho \rangle_{\mathrm{g}})]^2} = \sqrt{\left(\frac{1}{N} \sum_i \ln(\varrho_i)^2 \right) - \ln(\langle \varrho \rangle_{\mathrm{g}})^2}. \tag{2}$$

The meaning of σ is that the statistical scattering of the ratios with respect to $\langle \varrho \rangle_{\mathrm{g}}$ is given by a multiplicative factor $e^{\pm\sigma}$. In the above equations, the ratio of the intensities of line i is $\varrho_i = I_A(i)/I_B(i)$ and N is the total number of lines in the set.

Another quantity often reported (for example in [12]) is the root mean square (RMS) error given by

$$\sigma_{\mathrm{RMS}} = \sqrt{\frac{1}{N} \sum_i \left(\frac{I_A(i) - I_B(i)}{I_B(i)} \right)} = \sqrt{\frac{1}{N} \sum_i (\varrho_i - 1)}, \tag{3}$$

which reduces to the previously defined σ if $\langle \varrho \rangle_{\mathrm{g}} = 1$ (no systematic bias) and $\varrho_i \approx 1$ (small dispersion). However, in the case where even a few ratios differ significantly from 1, the analysis in terms of σ_{RMS} may give unreasonable results; in particular, this quantity is not symmetric with respect to inversion of the ratio I_A/I_B to I_B/I_A.

4. Comparisons with published data

Since the comparison with previous data highlighted a number of issues, the comparison below is given in an order designed to best illustrate these.

The BT2 water line list [21] was originally created using the DMS of Schwenke and Partridge [35] and the same FIS3 PES [19] used in this work. As can be seen from Table 1 and from Fig. 2, our line intensities agree closely with the BT2 ones. Our allowed lines are systematically 0.3% stronger that BT2 ones, independently of the absolute intensity of the line. On the other hand for forbidden lines our lines become increasingly stronger than the BT2 ones as the absolute intensity of the line decreases. The difference grows to about 2% for intensities of 10^{-28} cm/molecule (see Fig. 2). These differences are probably not significant when compared with other differences discussed below and are a consequence of the different underlying dipole surfaces used in the calculations. A more detailed comparison between the CVR and Schwenke and Partridge surfaces has been given elsewhere [20].

Next we consider the 2004 version of the HITRAN database [22], which contains a mixture of experimentally measured and computed lines. Our lines are, globally, more intense than HITRAN's by about 2–3%. If we exclude this systematic difference from the analysis then our lines and HITRAN's show differences of about 1 – 2% for medium and strong lines ($I > 10^{-24}$ cm/molecule). The weak forbidden lines show a much greater scatter, about 30% with respect to ours (see Table 1 and Fig. 3). This large deviation for the weak lines is dominated by a small set of about 40 lines which deviate very significantly from the computed values. These lines all lie outside the range of Fig. 3. All these lines come from measurements by Toth [34] (Rothman LS, private communication). Table 2 lists all the outlying HITRAN lines whose ratio to ours is less than 0.80 or more than 1.20, i.e. all the lines not present in Fig. 3. We note that in the cases where the intensity of these lines are also given by JPL, our results are all well within 10% of the JPL values. We regard the intensities given in HITRAN for the lines listed in Table 2 as likely to be wrong.

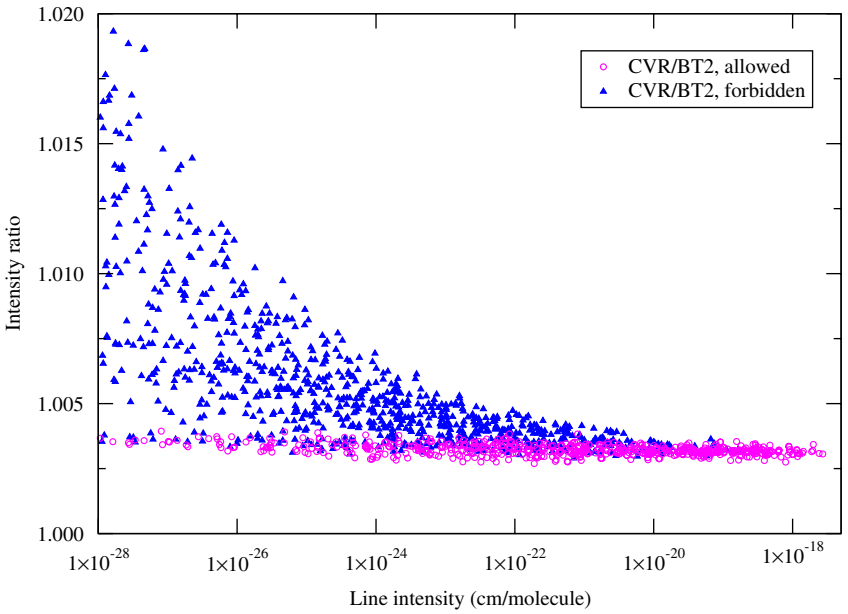

Fig. 2. Comparison of differences in the line intensities computed in this work and as part of the BT2 line list [21].

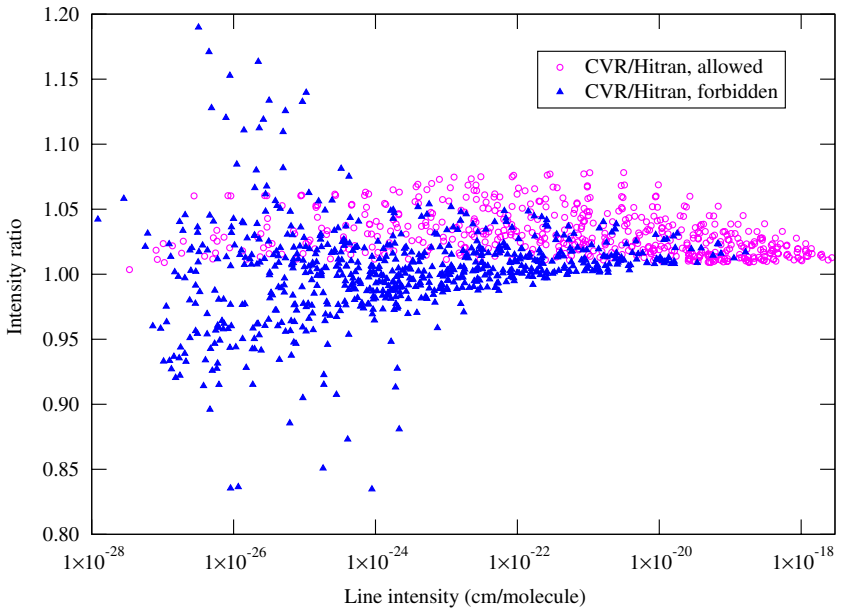

Fig. 3. Comparison of differences in the line intensities computed in this work and given in the HITRAN database [22]. The 37 outliers not displayed in the plot are listed in Table 2.

The JPL database was obtained from its Internet website [33] on 26 February 2007. We note that the database is periodically updated and, in fact, the version available on-line at the time of writing is different from the one used in the following analysis. Lines in the database are reported for a temperature of 300 K instead of 296 K and are expressed in different units. To convert them into the same format used for our computation the procedure outlined in HITRAN documentation [36] was followed. In particular, we used formula (11) of the above-mentioned reference to compute the temperature correction from 300 to 296 K. The

Table 2
Outliers in the HITRAN database [22]

Upper			Lower			Wavenumber	Intensities			Ratios	
J	K_a	K_c	J	K_a	K_c		CVR	HITRAN	JPL	HITRAN	JPL
10	9	2	9	0	9	1551.085	2.97E-30	2.07E-27	–	0.001	–
15	15	0	14	12	3	1182.460	3.91E-30	2.18E-27	–	0.002	–
10	10	1	9	3	6	1418.909	1.30E-29	2.07E-27	–	0.006	–
15	14	1	14	11	4	1167.519	5.01E-29	4.69E-27	–	0.011	–
8	8	0	7	1	7	1202.552	3.80E-28	1.04E-26	–	0.036	–
8	8	1	8	1	8	1044.879	1.73E-28	2.13E-27	–	0.081	–
10	8	3	10	1	10	1139.750	2.71E-28	3.32E-27	–	0.082	–
10	10	0	9	5	5	1226.874	9.70E-28	2.22E-27	–	0.437	–
8	7	1	8	0	8	846.631	2.03E-26	3.94E-26	1.87E-26	0.514	1.084
9	8	1	9	1	8	930.715	1.23E-26	2.35E-26	1.16E-26	0.523	1.060
9	9	1	9	4	6	884.553	1.79E-27	2.96E-27	1.83E-27	0.603	0.977
9	9	0	9	4	5	865.188	5.79E-27	9.47E-27	5.96E-27	0.612	0.972
9	7	3	8	0	8	1066.522	1.22E-25	1.59E-25	–	0.769	–
9	9	0	8	4	5	1102.727	3.79E-26	4.89E-26	–	0.773	–
14	7	8	14	2	13	936.485	1.45E-26	1.18E-26	1.37E-26	1.234	1.063
15	7	8	14	2	13	1301.254	3.63E-26	2.94E-26	–	1.236	–
8	8	1	7	3	4	946.645	4.00E-25	3.23E-25	4.15E-25	1.238	0.964
14	9	5	13	4	10	1259.199	7.49E-27	6.03E-27	–	1.243	–
14	8	7	14	3	12	913.426	8.06E-27	6.35E-27	8.30E-27	1.268	0.970
8	8	0	7	3	5	972.320	1.16E-25	8.74E-26	1.19E-25	1.327	0.970
15	8	7	14	3	12	1273.539	2.73E-26	2.05E-26	–	1.329	–
13	7	7	12	0	12	1369.283	7.23E-27	5.22E-27	–	1.386	–
14	6	9	14	1	14	1011.417	8.70E-27	6.19E-27	–	1.406	–
11	10	1	10	5	6	1254.071	6.05E-27	4.29E-27	–	1.411	–
13	8	6	12	1	11	1353.205	6.52E-27	4.53E-27	–	1.440	–
12	8	5	11	1	10	1288.670	4.55E-26	3.15E-26	–	1.445	–
11	7	4	11	0	11	994.832	1.81E-26	1.24E-26	–	1.458	–
15	9	6	14	4	11	1299.284	8.00E-27	5.38E-27	–	1.487	–
15	5	10	15	0	15	1002.470	3.57E-27	2.33E-27	–	1.531	–
7	7	0	7	0	7	808.567	2.83E-26	1.84E-26	2.65E-26	1.538	1.067
9	9	1	8	4	4	1093.653	1.29E-26	8.17E-27	–	1.579	–
12	9	4	11	2	9	1341.999	7.25E-27	3.69E-27	–	1.965	–
15	6	9	14	1	14	1399.500	1.09E-26	4.94E-27	–	2.205	–
14	7	8	13	0	13	1457.737	5.91E-27	2.43E-27	–	2.436	–
8	8	1	7	1	6	1084.803	2.21E-26	3.13E-27	–	7.052	–

The reported wavenumbers (in cm^{-1}) are computed ones. All intensities are in cm/molecule and refer to 296 K and to 100% of $H_2{}^{16}O$ (i.e. HITRAN intensities have been divided by the isotopic abundance of $H_2{}^{16}O$, 0.997317. JPL data [33], where available and converted to the same form as used by HITRAN, are reported for comparison. Ratios are given as Intensity(our)/Intensity(other). Lines whose calculated intensities are weaker/stronger than JPL ones are listed in the upper/lower portion of the table.

uncertainty of this formula depends on the molecule and, according to the quoted reference, should not exceed 2%. As an independent check we used the BT2 line list to calculate another set of lines at 300 K and then compared the intensity ratios $I_{BT2}(300K)/I_{BT2}(296K)$ with those predicted by the aforementioned formula. This comparison was done for the pure rotational lines in the (0 0 0) band up to 3500 cm^{-1}. The conclusion was that the formula reproduces the computed $I_{BT2}(300\,K)/I_{BT2}(296\,K)$ ratios extremely accurately (within a factor of $\pm 0.04\%$). We can thus very safely rely on the formula as any eventual error introduced by it would be about 100 times smaller than the intrinsic uncertainty of the original data.

Fig. 4 compares our intensities with those given in the JPL catalogue. Besides the larger than expected differences, there also appear to be systematic structures in the comparison. Fig. 5 gives an alternative comparison of the same data, this time as a function of wavenumber. This figure shows a series of remarkable systematic structures which cannot be explained by any likely error in our calculations. None of the other

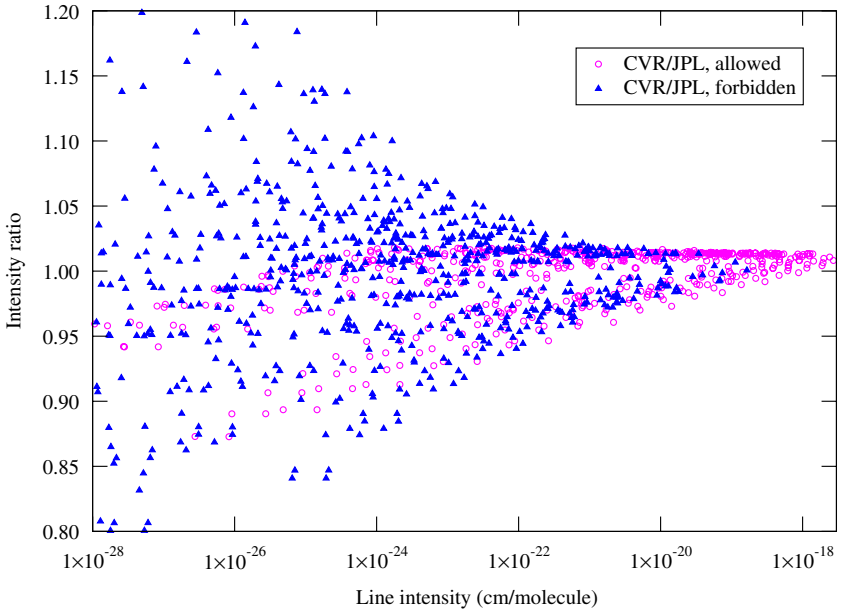

Fig. 4. Comparison of differences in the line intensities computed in this work and given in the JPL database [33].

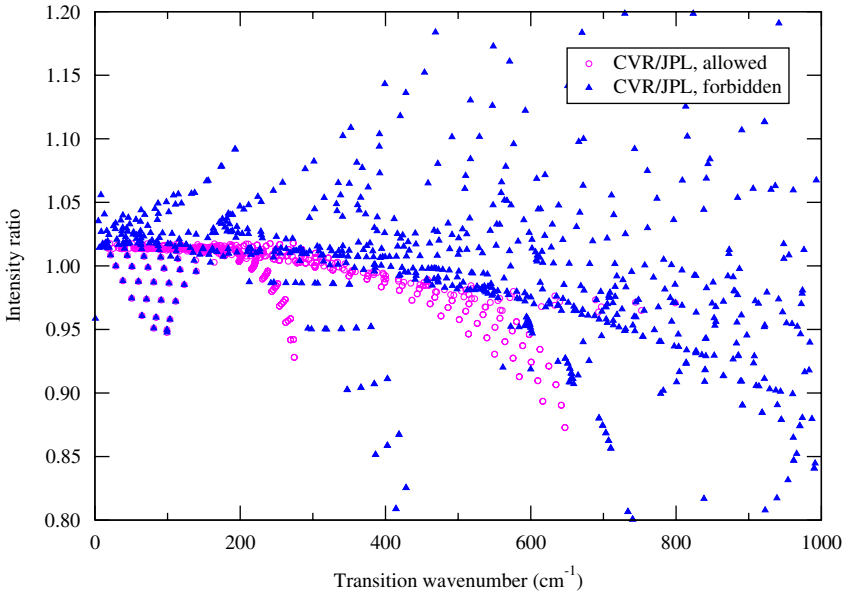

Fig. 5. Comparison of line intensities with lines form the JPL database [33] as a function of the transition wavenumber.

comparisons gave similar structures when plotted as a function of wavenumber. The discrepancies can also be studied in function of one of the rotational quantum numbers, for example, J_{upper}; analysis shows that, for the lines plotted in Figs. 4 and 5, the scatter in the ratios increases systematically with J_{upper}, with nearly all ratios lying within the range given by $1 \pm (J_{\text{upper}}/30)^2$.

While for strong lines JPLs are about 1% weaker than ours, as the lines get weaker, JPLs become comparatively stronger so that for weak lines the discrepancy can be up to about 20%. This seems to be due to a systematic error in the catalogue. In the case of forbidden lines weaker than about 10^{-28} cm/molecule there are several lines where the JPL values disagree strongly with the computed ones. Table 3 lists the 63 outliers whose intensity ratios do not lie in the range 1 ± 0.2.

Table 3
Outliers in the JPL catalogue [33]

Upper			Lower			Wavenumber	Intensities			Ratios	
J	K_a	K_c	J	K_a	K_c		CVR	JPL	HITRAN	JPL	HITRAN
12	9	3	13	2	12	990.342	5.50E-34	3.10E-32	–	0.018	–
14	11	4	15	4	11	927.484	2.46E-34	1.04E-32	–	0.024	–
15	15	0	15	12	3	817.132	4.07E-32	1.34E-31	–	0.303	–
15	15	1	15	12	4	817.132	1.36E-32	4.48E-32	–	0.303	–
14	14	0	14	11	3	794.896	4.25E-31	8.37E-31	–	0.508	–
14	14	1	14	11	4	794.896	1.27E-30	2.51E-30	–	0.508	–
15	14	2	15	11	5	804.711	3.02E-31	5.85E-31	–	0.517	–
15	14	1	15	11	4	804.711	9.07E-31	1.76E-30	–	0.517	–
15	13	3	15	10	6	782.916	3.65E-30	5.33E-30	–	0.684	–
15	13	2	15	10	5	782.914	1.09E-29	1.60E-29	–	0.684	–
14	13	2	14	10	5	775.327	2.47E-29	3.60E-29	–	0.685	–
14	13	1	14	10	4	775.326	8.22E-30	1.20E-29	–	0.685	–
13	13	1	13	10	4	767.217	1.04E-29	1.51E-29	–	0.686	–
13	13	0	13	10	3	767.216	3.12E-29	4.54E-29	–	0.686	–
14	11	3	15	6	10	728.915	3.56E-32	5.04E-32	–	0.705	–
13	11	3	14	4	10	950.270	6.79E-33	9.54E-33	–	0.712	–
13	11	2	14	6	9	746.302	1.40E-31	1.93E-31	–	0.725	–
12	11	2	13	4	9	978.535	3.20E-32	4.35E-32	–	0.736	–
13	11	3	14	6	8	729.674	6.30E-32	8.35E-32	–	0.754	–
14	11	4	15	6	9	699.188	1.67E-31	2.16E-31	–	0.775	–
12	11	1	13	6	8	764.269	3.81E-32	4.91E-32	–	0.777	–
14	14	1	15	11	4	432.089	6.38E-33	8.17E-33	–	0.781	–
14	14	0	15	11	5	432.089	2.13E-33	2.72E-33	–	0.781	–
12	11	2	13	6	7	755.941	1.40E-31	1.77E-31	–	0.789	–
15	12	4	15	9	7	751.667	3.15E-29	4.00E-29	–	0.789	–
15	12	3	15	9	6	751.630	9.46E-29	1.20E-28	–	0.789	–
14	12	2	14	9	5	746.205	8.86E-29	1.12E-28	–	0.795	–
14	12	3	14	9	6	746.216	2.66E-28	3.34E-28	–	0.795	–
14	5	9	14	0	14	910.028	9.08E-27	7.56E-27	9.02E-27	1.201	1.006
13	4	9	14	1	14	460.415	2.45E-26	2.03E-26	2.60E-26	1.209	0.942
13	7	6	14	2	13	600.089	1.75E-27	1.45E-27	1.90E-27	1.212	0.922
11	6	5	12	1	12	586.262	1.98E-26	1.60E-26	2.10E-26	1.237	0.943
13	9	5	14	2	12	796.910	2.45E-30	1.98E-30	–	1.239	–
9	7	3	10	0	10	696.077	8.67E-28	6.96E-28	–	1.245	–
11	8	4	12	1	11	747.666	9.65E-29	7.69E-29	–	1.255	–
13	5	9	14	0	14	513.114	5.96E-27	4.75E-27	6.40E-27	1.256	0.932
14	7	7	15	2	14	635.313	1.28E-28	9.89E-29	–	1.291	–
14	4	10	15	1	15	522.683	1.52E-27	1.16E-27	1.65E-27	1.315	0.920
12	6	6	13	1	13	630.914	1.71E-27	1.28E-27	1.83E-27	1.338	0.936
10	7	4	11	0	11	727.273	1.48E-27	1.11E-27	1.48E-27	1.340	1.002
12	8	5	13	1	12	771.235	1.18E-28	8.80E-29	–	1.347	–
13	12	2	14	7	7	821.430	1.79E-33	1.31E-33	–	1.366	–
14	5	10	15	0	15	560.058	3.78E-27	2.76E-27	4.13E-27	1.368	0.914
11	10	2	12	3	9	866.912	2.39E-32	1.60E-32	–	1.494	–
11	7	5	12	0	12	764.020	1.99E-28	1.33E-28	–	1.499	–
13	8	6	14	1	13	799.968	1.20E-29	7.96E-30	–	1.505	–
13	6	7	14	1	14	683.008	1.03E-27	6.80E-28	1.10E-27	1.516	0.933
11	9	2	12	2	11	965.684	2.61E-32	1.70E-32	–	1.533	–
8	8	0	9	1	9	868.843	1.94E-30	1.23E-30	–	1.569	–
12	7	6	13	0	13	806.198	1.81E-28	1.01E-28	–	1.793	–
14	8	7	15	1	14	833.684	8.37E-30	4.61E-30	–	1.815	–
14	10	5	15	3	12	842.135	1.52E-31	8.37E-32	–	1.820	–
14	6	8	15	1	15	743.278	5.32E-29	2.85E-29	–	1.867	–
9	8	1	10	1	10	895.275	8.55E-30	4.52E-30	–	1.892	–
14	12	2	15	7	9	807.417	5.39E-34	2.30E-34	–	2.345	–

Table 3 (*continued*)

Upper			Lower			Wavenumber	Intensities			Ratios	
J	K_a	K_c	J	K_a	K_c		CVR	JPL	HITRAN	JPL	HITRAN
13	7	7	14	0	14	853.646	1.41E-29	5.76E-30	–	2.451	–
10	8	2	11	1	11	927.197	1.83E-30	6.62E-31	–	2.762	–
14	12	3	15	7	8	802.494	1.43E-33	4.27E-34	–	3.341	–
9	9	0	10	2	9	931.832	1.39E-31	3.24E-32	–	4.283	–
14	7	8	15	0	15	906.143	8.06E-30	1.76E-30	–	4.568	–
10	10	1	11	3	8	888.612	7.85E-33	1.15E-33	–	6.832	–
11	8	3	12	1	12	964.461	1.94E-30	2.39E-31	–	8.110	–
10	9	1	11	2	10	946.124	4.36E-32	2.31E-33	–	18.906	–

The reported wavenumbers (in cm^{-1}) are computed ones. All intensities are in cm/molecule and refer to 296 K. HITRAN data [22] are reported for comparison. Ratios are given as Intensity(our)/Intensity(other). Lines whose calculated intensities are weaker/stronger than JPL ones are listed in the upper/lower portion of the table.

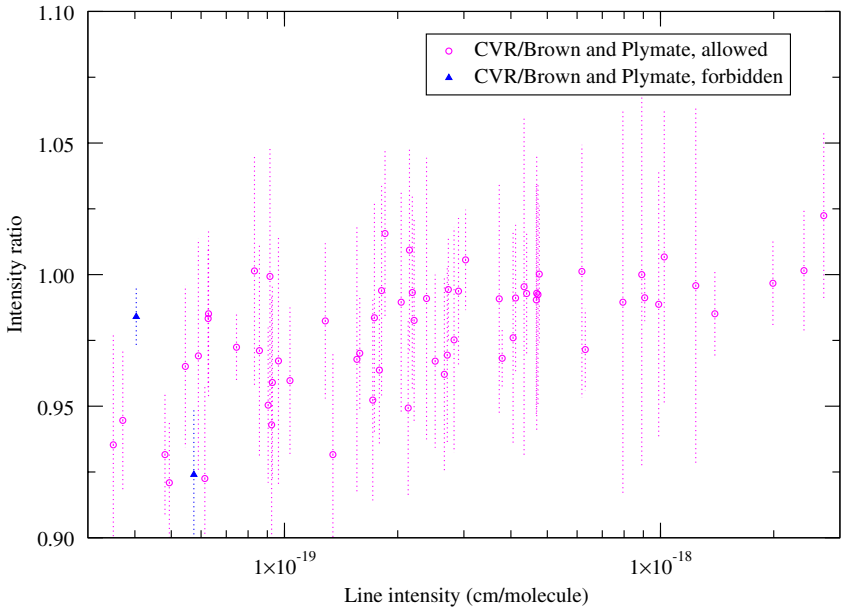

Fig. 6. Comparison of differences in the line intensities computed in this work and measured by Brown and Plymate [7]. The lines lie energetically between 55 and 328 cm^{-1}.

Outliers whose JPL intensities are stronger than calculated ones are all very weak lines not present in HITRAN (or indeed anywhere else that we found); in particular, JPL lines stronger by more than a factor of 2 with respect to calculated ones have absolute intensities of about 10^{-31} cm/molecule or less. Some of the outliers whose JPL intensities are weaker than calculated ones are present in HITRAN and for these our results are within 10% of those given by HITRAN. Again, all lines that differ with calculated ones by more then a factor of 2 are extremely weak lines with intensities less than 10^{-30} cm/molecule.

The systematic differences between our calculations and the JPL catalogue data are not confined to the outliers. Indeed they would appear to be shown by nearly all the higher J $H_2{}^{16}O$ pure rotation data reported by JPL.

Brown and Plymate [7] published a list of 67 strong lines within the ground vibrational levels (65 allowed and 2 forbidden; see Fig. 6). Fifty-five of these lines are compared by Coudert with his semi-empirical

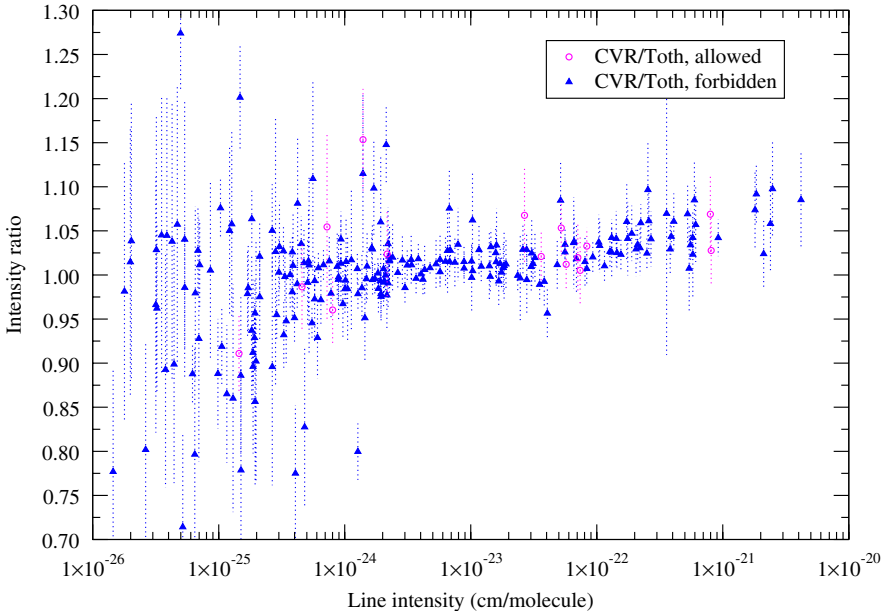

Fig. 7. Comparison of differences in line intensities computed in this work and measured by Toth [9,34]. The lines lie energetically between 590 and 1286 cm^{-1}, with most in the 600–800 cm^{-1} region.

calculations. Brown and Plymate measured relative, not absolute, intensities which were normalised to the HITRAN 1992 values. Their reported lines are systematically 2% stronger than our calculated ones, a reflection of the HITRAN values used for the normalisation, with a scatter of 2%. The experimental lines become comparatively stronger as their absolute intensity decreases, with differences of up to about 7% for the weakest lines reported ($I \sim 3 \times 10^{-20}$ cm/molecule). If we disregard the constant multiplicative factor due to the normalisation, our calculated values almost always agree with the measurements within the reported experimental uncertainty. Brown and Plymate's lines are systematically stronger than Coudert's by 4% with a scatter of 2%. Our results are therefore essentially in agreement with the data presented by Coudert.

Toth measured the intensity of water transitions at wavenumbers above 500 cm^{-1}: some lines reported in [9] and other lines available on-line from [34]. Fig. 7 compares our calculations with Toth's measurement. Our lines are, on average, about 3% stronger than Toth's. Outliers which differ by more than 20% are given in Table 4; for all of these lines our intensities are within 10% of those given in HITRAN. However, for most lines our calculations agree within the stated experimental uncertainties. On the other hand, Coudert's [12] calculated line intensities for a selection Toth's lines (22 lines, some of them with $J > 15$) are 2% stronger but with a scatter of 9%.

Rinsland et al. [6] measured the intensity of water transitions at wavenumbers between 802 and 1043 cm^{-1}. Of these, 35 lines correspond to rotational transitions in the vibrational ground state with $J < 15$. Fig. 8 compares our calculations with the measurement. The trend is the same as the one identified in the analysis of Toth's data relative to medium-strength lines: our lines are about 3% stronger than the reported ones, with a scatter of about 2%. However, the reported experimental uncertainties are in general larger (sometimes much larger) that the discrepancy with our calculation, so that we are fully consistent with the limited experimental data analysed.

5. Summary

We present a line list of pure rotational transitions for water, data which have been made available electronically. The aim of this list is not to present transition frequencies, as these can be measured to much higher accuracy than our calculations, but to present transition intensities. We believe these calculated

Table 4
Outliers in Toth's database [9,34]

Upper			Lower			Wavenumber	Intensities			Ratios	
J	K_a	K_c	J	K_a	K_c		CVR	Toth	HITRAN	Toth	HITRAN
12	10	3	11	5	6	1267.714	6.86E-27	8.31E-26	7.12E-27	0.083	0.964
12	12	1	11	9	2	1025.957	1.87E-26	4.68E-26	2.04E-26	0.399	0.915
12	10	3	12	7	6	653.942	8.18E-26	2.01E-25	8.08E-26	0.407	1.012
14	9	6	13	4	9	1151.542	4.99E-26	1.02E-25	4.61E-26	0.489	1.082
10	7	3	10	0	10	939.860	1.33E-26	2.57E-26	1.28E-26	0.518	1.040
12	9	4	11	4	7	1133.614	1.15E-25	2.19E-25	1.08E-25	0.526	1.063
11	7	5	10	0	10	1207.304	5.19E-26	7.26E-26	5.26E-26	0.714	0.986
9	8	2	8	3	5	959.600	4.06E-25	5.24E-25	4.65E-25	0.775	0.873
14	7	8	14	2	13	936.485	1.45E-26	1.87E-26	1.18E-26	0.777	1.234
15	5	11	15	2	14	638.337	1.50E-25	1.93E-25	1.52E-25	0.779	0.991
15	10	5	14	7	8	1018.937	6.46E-26	8.11E-26	6.23E-26	0.797	1.037
15	7	9	14	2	12	1073.334	1.48E-25	1.23E-25	1.46E-25	1.201	1.009
13	9	4	12	4	9	1222.801	4.98E-26	3.91E-26	4.49E-26	1.274	1.109
13	8	6	13	3	11	879.747	8.86E-27	6.74E-27	7.69E-27	1.315	1.153
10	8	3	9	1	8	1175.191	9.48E-26	6.66E-26	1.05E-25	1.424	0.905
11	9	2	10	4	7	1159.049	1.06E-25	6.78E-26	9.26E-26	1.557	1.140
15	6	10	14	1	13	1115.379	1.72E-25	1.06E-25	1.72E-25	1.618	1.000
10	9	2	9	4	5	1110.970	9.35E-26	5.28E-26	8.25E-26	1.770	1.133

The reported wavenumbers (in cm^{-1}) are computed ones. All intensities are in cm/molecule and refer to 296 K. HITRAN 2004 data [22] are reported for comparison. Ratios are given as intensity(our)/intensity(other). Lines whose calculated intensities are weaker/stronger than JPL ones are listed in the upper/lower portion of the table.

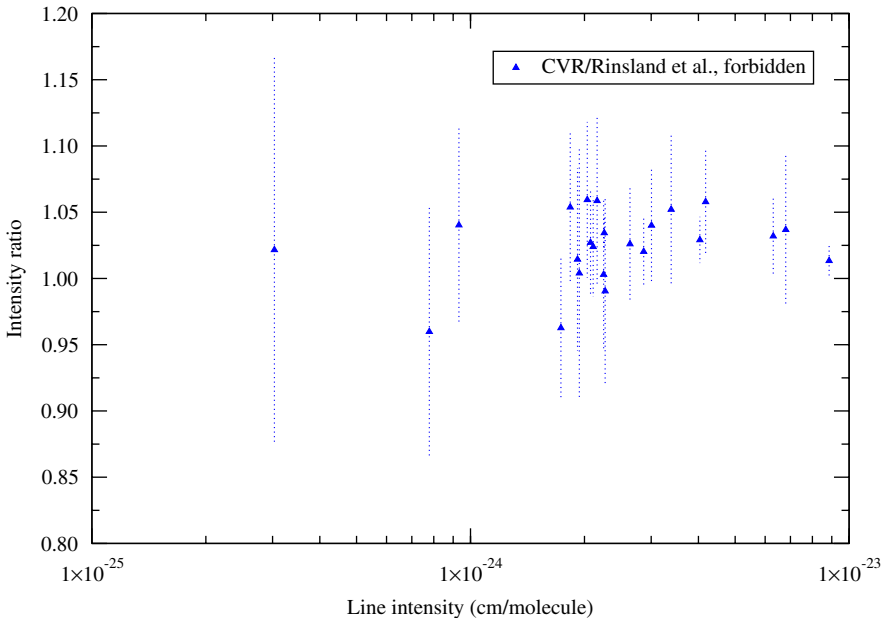

Fig. 8. Comparison of differences in line intensities computed in this work and measured by Rinsland et al. [6]. The lines lie energetically between 802 and 1042 cm^{-1}.

intensities to be accurate over a large dynamic range. Our calculated intensities should be reliable within 5% of the true value in the worst case, and our line list therefore provides intensity data when reliable experimental values are not available.

We provide the line list as two separate files, one for allowed and one for forbidden lines. As an example of the format used we list the first record of the allowed-lines list:

J'	K'_a	K'_c	J''	K''_a	K''_c	$\overline{\nu}_{\rm th}$	$\overline{\nu}_{\rm JPL}$	I	A	$S(i\rightarrow f)$
7	5	2	6	6	1	14.782474	14.777500	1.511E-23	5.562E-06	3.315E-01

where J, K_a and K_c are the rotational quantum numbers for the upper and lower state, respectively, $\overline{\nu}_{\rm th}$ is the theoretical (computed) transition wavenumber in $\rm cm^{-1}$, $\overline{\nu}_{\rm JPL}$ is the transition wavenumber as reported by the JPL catalogue (when available), I is the line intensity in cm/molecule at 296 K, A is the Einstein coefficient for the transition in $\rm s^{-1}$ and finally $S(i\rightarrow f)$ is the 'line strength' in D^2 for all magnetic components of the line. As there are several definitions of 'line strength' we note that the reported $S(i\rightarrow f)$ is linked to the transition intensity I by

$$I(\omega)=\frac{4.162034\times10^{-19}\omega g_i[{\rm e}^{-E''/k_BT}-{\rm e}^{-E'/k_BT}]}{Q(T)}\times S(i\rightarrow f), \tag{4}$$

where g_i is the nuclear-spin weighting times the degeneracy weighting, ω is the transition wavenumber, E' and E'' are the energies of the upper and lower levels of the transition, T is the temperature and $Q(T)$ is the partition function.

Our line intensities have been been compared with those available in the literature and found to be in good agreement with the semi-empirical results of Coudert [12] and the forbidden-line measurements of Toth [9]. Agreement with the latest version of the HITRAN database [22] is also reasonable, although there are a small number of weaker lines for which we suggest there are significant errors in the intensities given by HITRAN. The situation regarding the JPL catalogue [33] is much less satisfactory; comparisons show a number of systematic differences even for lines which have been well characterised and cannot be a consequence of our calculations. We suggest that the water data in this catalogue should be systematically re-evaluated. This is particularly true because JPL is the major supplier of data for space missions, several of which have observing pure rotational transitions of water as a major objective [2,39–41].

It is difficult to give error bars for calculated data such as those presented here as the errors are essentially all systematic. However, it is possible to make some comments about the probable source and magnitude of the errors in our predicted transition intensities. As discussed above the major source of error for nearly all lines will be associated with imperfections in the CVR dipole moment surface used in this work. This surface overestimates the equilibrium dipole moment by 0.013 D or 0.7% [20]. In the rigid rotor approximation the intensity of allowed transitions depends on the square of this dipole, so CVR should give transitions which are about 1.4% too strong. Comparisons given above with HITRAN, Toth and Coudert all suggest that our lines are indeed slightly too intense; it is possible that reducing their intensity by 1.4% would lead to more accurate predictions but we have not done this here because it is not clear whether this is the appropriate procedure in all cases and in any case 1.4% is less than the experimental error on any of the measured data we compare with.

Finally it should be noted that we have confined ourselves here to the study of pure rotational transitions involving $J\leqslant15$ and within the vibrational ground state. These are the transitions of importance for studies at room temperature or below. Of course in hotter environments many more pure rotational transitions involving both higher J's and transitions within excited vibrational states become important [37,38]. Information on these transitions, and indeed other shorter wavelength vibration–rotation transitions, can be found in the BT2 line list [21].

Acknowledgements

We thank Iouli Gordon and Larry Rothman for helpful discussions. We also thank Brian Drouin, Linda Brown, Laurent Coudert and Robert Toth for their comments on our manuscript. This work was supported by the QUASAAR EU Marie Curie research training network and was performed as part of IUPAC task group 2004-035-1-100 on a database of water transitions from experiment and theory.

Appendix A. Supplementary data

Supplementary data associated with this article can be found in the online version at doi:10.1016/j.jqsrt.2007.09.015.

References

[1] Bernath PF. The spectroscopy of water vapour: experiment, theory and applications. Phys Chem Chem Phys 2002;4:1501–9.
[2] Kessler MF, Steinz JA, Anderegg ME, Clavel J, Drechsel G, Estaria P, et al. The Infrared Space Observatory (ISO) mission. Astron Astrophys 1996;315:L27–31.
[3] Melnick GJ, et al. The submillimeter wave astronomy satellite: science objectives and instrument description. Astrophys J 2000;539:L77–85.
[4] Perrin A, Puzzarini C, Colmont JM, Verdes C, Wlodarczak G, Cazzoli G, et al. Molecular line parameters for the "MASTER" (millimeter wave acquisitions for stratosphere/troposphere exchange research) database. J Atmos Chem 2005;51:161–205.
[5] Hall RT, Dowling JM. Pure rotational spectrum of water vapor. J Chem Phys 1967;47:2454–61;
Hall RT, Dowling JM. Pure rotational spectrum of water vapor. J Chem Phys 1971;54:4968 (errata).
[6] Rinsland CP, Goldman A, Smith MAH, Devi VM. Measurements of Lorentz air-broadening coefficients and relative intensities in the $H_2{}^{16}O$ pure rotational and v_2 bands from long horizontal path atmospheric spectra. Appl Opt 1991;30:1427–38.
[7] Brown LR, Plymate C. H_2-broadened $H_2{}^{16}O$ in four infrared bands between 55 and 4045 cm^{-1}. JQSRT 1996;56:263–82.
[8] Toth RA. Water vapour measurements between 590 and 2582 cm^{-1}: line positions and strengths. J Mol Spectrosc 1998;190:379–96.
[9] Toth RA. Air- and N_2-broadening parameters of water vapour: 604 to 2271 cm^{-1}. J Mol Spectrosc 2000;201:218–43.
[10] Chen P, et al. Submillimeter-wave measurement and analysis of the ground and $v_2 = 1$ states of water. Astrophys J Suppl Ser 2000;128:371–85.
[11] Coudert LH. Analysis of the line positions and line intensities in the v_2 band of the water molecule. J Mol Spectrosc 1997;181:246–73.
[12] Coudert LH. Line frequency and line intensity analyses of water vapour. Mol Phys 1999;96:941–54.
[13] Sarka K, Demaison J. Computational molecular spectroscopy. New York: Wiley; 2000 [Chapter 8].
[14] Tennyson J. Calculating the vibration–rotation spectrum of water. Phys Scr 2006;76:C53–6.
[15] Polyansky OL, Császár AG, Shirin SV, Zobov NF, Barletta P, Tennyson J, et al. High-accuracy ab initio rotation–vibration transitions for water. Science 2003;299:539–42.
[16] Miani A, Tennyson J. Can ortho-para transitions for water be observed? J Chem Phys 2004;120:2732–9.
[17] Tennyson J. Astronomical spectroscopy. Imperial College Press; 2005 (Chapter 5).
[18] Tennyson J, Kostin MA, Barletta P, Harris GJ, Polyansky OL, Ramanlal J, et al. DVR3D: a program suite for the calculation of rotation–vibration spectra of triatomic molecules. Comput Phys Commun 2004;85:116–63.
[19] Shirin SV, Polyansky OL, Zobov NF, Barletta P, Tennyson J. Spectroscopically determined potential energy surface of $H_2{}^{16}O$ up to 25000 cm^{-1}. J Chem Phys 2003;118:2124–9.
[20] Lodi L, Tolchenov FN, Tennyson J, Lynas-Gray AE, Shirin SV, Zobov NF, et al. A new ab initio ground state dipole moment surface for the water molecule. J Chem Phys, in press.
[21] Barber RJ, Tennyson J, Harris GJ, Tolchenov RN. A high accuracy computed water line list. Mon Not R Astron Soc 2005;000:1–9.
[22] Rothman LS, Jacquemart D, Barbe A, Benner DC, Birk M, Brown LR, et al. The HITRAN 2004 molecular spectroscopic database. JQSRT 2005;96:139–204.
[23] Tennyson J, Barletta P, Kostin MA, Polyansky OL, Zobov NF. Ab initio rotation–vibration energy levels of triatomics to spectroscopic accuracy. Spectrochim Acta A 2002;58:663–72.
[24] Voronin BA, Naumenko OV, Tolchenov RN, Tennyson J, Folly S, Coheur P-F, et al. HDO absorption spectrum above 11500 cm^{-1}: assignment and dynamics. J Mol Spectrosc 2007;244:87–101.
[25] Barletta P, Shirin SV, Zobov NF, Polyansky OL, Tennyson J, Valeev EF, et al. CVRQD ab initio ground-state adiabatic potential energy surfaces for the water molecule. J Chem Phys 2006;125:204307. [18pp].
[26] Schryber JH, Miller S, Tennyson J. Computed infrared-absorption properties of hot-water vapour. JQSRT 1995;53:373–80.
[27] The HITRAN 2004 database is available electronically from: ⟨http://www.cfa.harvard.edu/hitran/⟩.
[28] Pickett HM, Poynter RL, Cohen EA, Delitsky ML, Pearson JC, Müller HSP. Submillimeter, millimeter, and microwave spectral line catalog. JQSRT 1998;60:883–90.
[29] Toth RA. Transition frequencies and absolute strengths of $H_2{}^{17}O$ and $H_2{}^{18}O$ in the 6.2 mm region. J Opt Soc Am B 1992;9:462–82.
[30] Pearson JC. Private communication. Pasadena CA, USA: Jet Propulsion Laboratory; 1999.
[31] Lanquetin R, Coudert LH, Camy-Peyret C. High-lying rotational levels of water: an analysis of the energy levels of the five first vibrational states. J Mol Spectrosc 2001;206:83–103.
[32] Flaud JM, Piccolo C, Carli B, Perrin A, Coudert LH, Teffo JL, et al. Molecular line parameters for the MIPAS (Michelson interferometer for passive atmospheric sounding) experiment. Atmos Ocean Opt 2003;16:172–81.
[33] The JPL catalog for water is available electronically from: ⟨http://spec.jpl.nasa.gov/ftp/pub/catalog/catdir.html⟩.
[34] Data is available from the 'MkIV Fourier Transform InfraRed (FTIR) Interferometer Atmospheric Chemistry Research Element' website: ⟨http://mark4sun.jpl.nasa.gov/⟩.

[35] Schwenke DW, Partridge H. Convergence testing of the analytic representation of an ab initio moment function for water: improved fitting yields improved intensities. J Chem Phys 2000;113:6592–7.
[36] Rothman LS, Gordon I. Steps for converting intensities from the JPL (or CDMS) catalog to HITRAN intensities. ⟨http://www.cfa.harvard.edu/hitran/Download/Units-JPLtoHITRAN.pdf⟩.
[37] Polyansky OL, Zobov NF, Viti S, Tennyson J, Bernath PF, Wallace L. Water on the Sun: line assignments based on variational calculations. Science 1997;277:346–9.
[38] Coheur P-F, Bernath PF, Carleer M, Colin R, Polyansky OL, Zobov NF, et al. A 3000 K laboratory emission spectrum of water. J Chem Phys 2005;122:074307. (8pp).
[39] Melnick GJ, Stauffer JR, Ashby MLN, Bergin EA, Chin G, Erickson NR, et al. The submillimeter wave astronomy satellite: science objectives and instrument description. Astrophys J Lett 2000;539:L77–86.
[40] Hjalmarson A, Bergman P, Biver N, Floren HG, Frisk U, Hasegawa T, et al. Recent astronomy highlights from the Odin satellite. Adv Space Res 2005;36:1031–47.
[41] Harwit M. The Herschel mission. Adv Space Res 2004;34:568–72.